16th ICAAR LISBOA 2020-2022

16th International Conference on
Alkali-Aggregate Reaction in Concrete
Lisboa | LNEC | Portugal | 31 May - 2 June 2022

http://icaar2020-2022.lnec.pt

Predicting the effect of SCMs on ASR in the accelerated mortar bar test with artificial neural networks

Maxime Ranger [1,2], Marianne Tange Hasholt [2], Ricardo Antonio Barbosa [3], Lene Højris Jensen [1]

(1) Danish Road Directorate, Hedehusene, Denmark, maxr@vd.dk

(2) Technical University of Denmark, Kongens Lyngby, Denmark

(3) Danish Technological Institute, Taastrup, Denmark

Abstract

Supplementary cementitious materials (SCMs) are an efficient way to both mitigate ASR and reduce the carbon footprint of concrete. Identifying possible new materials and assessing their suitability regarding ASR have become major issues, since the amount of traditional SCMs such as fly ash is declining. Accelerated mortar bar test has been widely used to test different materials with various replacement levels, and a substantial amount of data is available in the literature. This study explores the possibility of using artificial neural networks to analyse this large dataset. Attention is drawn on the relationship between the chemical composition of the binder and the reduction in expansion brought by the addition of SCMs, compared to the reference mixes with cement only. Using a baseline case with only the CaO and SiO_2 contents of the binder as inputs, one can see that the individual addition of other compounds (Al_2O_3, Fe_2O_3, MgO, SO_3 and Na_2O_{eq}) does improve the neural network performance. Combining them altogether improves the performance even further, although the assumption of independence of inputs may no longer be valid. After training, the artificial neural network is able to predict with a relatively good accuracy the SCM effect: the reduction in expansion is successfully predicted within ± 20 percentage points for more than 90 % of the dataset. However, uncertainties remain on the quantitative effect of each oxide, which could be investigated further by performing other types of regression on the same dataset. Besides, increasing the dataset size to fully exploit the potential of artificial neural networks and investigating methods to shed light on the input-output relationship are also promising leads to strengthen the analysis.

Keywords: *accelerated mortar bar test, alkali-silica reaction, artificial neural network, supplementary cementitious materials.*

1. INTRODUCTION

Supplementary cementitious materials (SCMs) play an important role in reducing the influence of concrete on global warming. Amongst all concrete constituents, cement has by far the largest CO_2 contribution, typically around 70 % [1]. Traditional SCMs such as fly ash, silica fume or GGBF slag provide good examples of circularity, by upcycling industrial by-products. As a twofold effect, they can both reduce the carbon footprint of concrete by substituting part of the cement and improve concrete durability. However, these materials come from industries emitting large amounts of CO_2, which are also at the core of environmental challenges. In Denmark, coal-fired power plants are currently phased out, which will make fly ash no longer available locally in the coming years. It is therefore necessary to find alternatives and assess their suitability.

Alkali-silica reaction (ASR) is one of the major concrete deterioration mechanisms that has been studied for more than 70 years. ASR is a chemical reaction taking place in the pore solution of concrete between alkali hydroxides (OH^-, Na^+ and K^+) and amorphous silica from aggregates dissolved at high pH [2]. The alkalis mostly come from cementitious materials, but some aggregates can also bring a significant contribution [3]. Traditional SCMs have proven to be an efficient way to mitigate deleterious ASR, and some extensive research have been carried out to document their effect [4]. One of the biggest challenges with ASR is the slow speed of reaction, as it can take some decades before seeing any sign of damage in field structures. Accelerated tests are therefore necessary to evaluate the ASR risk within a reasonable amount of time prior to construction. Two main accelerated tests have been used so far: the accelerated mortar bar test, AMBT (ASTM C1260/C1567, CAN/CSA A23.2-25A/28A, RILEM AAR-2), and the concrete prism test, CPT (ASTM C1293, CAN/CSA A23.2–14A, RILEM AAR-3). Although these tests were initially developed for assessing aggregate reactivity, they have also been used to

evaluate the effect of SCMs on the ASR expansion. While the literature provides numerous test results for both AMBT and CPT with traditional SCMs, new SCMs have mostly been tested only with AMBT so far.

New SCMs, such as calcined clays, biomass ashes, sewage sludge ashes or waste construction materials (glass, brick) may have a higher alkali content than traditional materials. Their diversity is also reflected by a wide range of chemical compositions. A few studies have focused on the relationship between the chemical composition of fly ashes and the expansion of mortar bars containing these materials in the AMBT [5, 6]. Attempts were made to correlate a chemical index, derived from the chemical composition, to the normalized expansion at 14 days by means of a non-linear regression analysis. This approach was subsequently applied to other types of SCMs [7, 8].

Regression analysis refers to problems where it is intended to make a qualitative prediction of a variable, which is dependent of independent inputs [9]. One traditional way of performing regression analysis is to find the mathematical function that represents the relationship between the inputs and the output the best. This can take the form of curve fitting, where the general form of the function is known but some fitting parameters have to be adjusted. However, nowadays machine learning offers new possibilities to analyse large datasets, almost without any assumption on the input-output relationship. Artificial neural network (ANN) is one type of modelling in machine learning and can be used for both classification and regression problems [10]. ANNs perform usually quite well for making predictions, and they also have the advantage of being easy to use once the model has been set, by changing the number of inputs for instance.

The objective of the present work is to investigate how the chemical composition of SCMs influences the expansion of mortar bars in the AMBT, even if the AMBT is considered as a rapid screening test that does not itself reliably predict the performance of concrete. This is done by performing regression on a large dataset with ANNs, which aims to find out what the generic relationship is and move from experimental measurements towards empirical generalization.

2. ARTIFICAL NEURAL NETWORKS

Machine learning has now become a well-known tool for analysing large datasets. Machine learning is typically divided into three categories: unsupervised learning, supervised learning and reinforced learning. Amongst these three, supervised learning is probably the most comparable to the usual learning process of the human brain [10]. This can be seen as an iterative process, based on the “learning from mistakes” principle. Given a problem, some inputs and the current knowledge, an attempt is made to solve the problem, and an answer is generated. Then, the answer is compared to the solution. If a difference is noticed, the way of processing the inputs is modified, and a new answer is proposed. This process continues until the difference between the answer and the solution is judged as acceptable.

In machine learning, the artificial neural network (ANN) approach is one of the tools that allow supervised learning. The following gives an overall description and introduction to how they operate, as well as the basis for the model developed later in this paper.

2.1 Structure of an ANN

The ANNs mimic the structure of the human brain. An ANN is made of three distinct parts: the input layer, the hidden layer(s) and the output layer. They can be identified as the dendrites, the synapses and the axon in a biological neuron [11]. In the ANN, each neuron is connected to all neurons of the subsequent layer, and a weight w_{ij} is associated to each connection. This structure can be seen in Figure 2.1.

The role of an artificial neuron is to classify inputs. A single input value is calculated by summing up all the weighted inputs connected to the neuron. Then, this value passes through a so-called activation function. In its simplest form, i.e. the step function, the activation function returns 0 if the input value is below a threshold limit, 1 otherwise. However, the step function is not appropriate for ANNs, because of the non-continuous gradient. For this reason, the sigmoid is often preferred as the default activation function [12]. To facilitate the classification process, an offset value can be added to the input value of the activation function. Such offset is called a bias, denoted as b_j. Biases are essentially giving one more degree of freedom in order to make the classification more accurate [11].

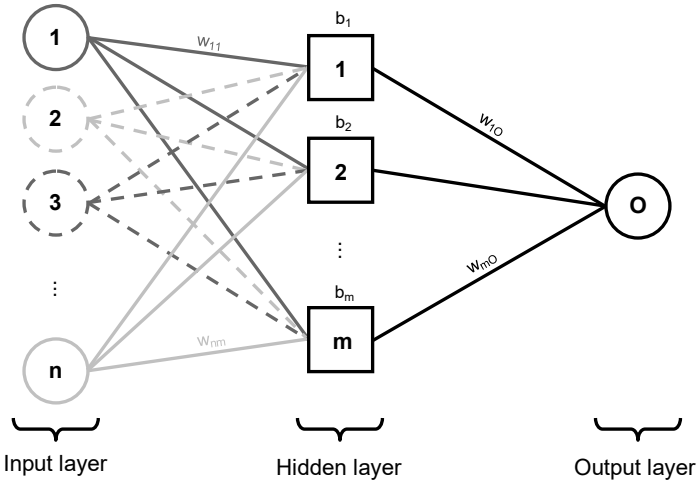

Figure 2.1: Structure of an artificial neural network, with a single hidden layer

Once data have gone through all hidden neurons, they reach the output layer. This process is referred to as forward propagation [11]. The calculated output is then compared to the real output, by means of a loss function. The minimization of the loss function is done through a process called backpropagation. Different methods exist, but the Levenberg-Marquardt algorithm has proven to be quite efficient for non-linear functions. In short, it consists of a combination between the steepest descent (stable but slow) and the Gauss-Newton (unstable but fast) algorithms, by means of an adaptive combination coefficient μ. The term adaptive refers to the fact that μ is updated after each iteration, typically by multiplying or dividing it by a fixed factor. As an example, if the performance improves between two iterations, μ is reduced, and the calculation scheme gets closer to the Gauss-Newton algorithm. On the other hand, if the performance does not improve enough, μ is increased and make the steepest descent part dominant [13].

2.2 Architecture

The ANN is somehow similar to a system of equations to solve. Let I, H and O be respectively the number of input neurons, hidden neurons and output neurons. The total number of unknows N_u is given by Equation (1). The number of equations N_{eq} depends on the number of training data points N_{tr}, via Equation (2).

$$N_u = (I + 1)\, H + (H + 1)\, O \tag{1}$$

$$N_{eq} = N_{tr}\, O \tag{2}$$

As any system of equations, it can only be solved if $N_u \leq N_{eq}$, which can also be expressed as a condition on the number of hidden neurons by means of Equation (3).

$$H \leq \frac{(N_{tr} - 1)\, O}{I + O + 1} \tag{3}$$

For a classical system of equations, the equality case in Equation (3) would correspond to a system with a unique solution. On the other hand, the strict inequality would result in an over-constrained system. However, when using an ANN, the relationship that contains the loss function is not an equality, but only a minimization relationship. Therefore, the solution depends on how many training data are available: the higher N_{tr}, the better the generalization. Thus, for ANNs it is often required that $N_u \ll N_{eq}$, so that Equation (3) will rather take the form of an inequality, as shown in Equation (4).

$$H \ll \frac{(N_{tr} - 1)\, O}{I + O + 1} \tag{4}$$

2.3 Training

During the training stage, supervised learning is performed. It consists in a succession of forward and back propagations on the training subset, each cycle being called an epoch. Thus, after each epoch, the weights and biases are updated to improve the training performance. In the meantime, the updated

ANN is applied to the validation subset, without backpropagation. The validation subset can therefore be used to test whether the ANN is trained enough or not [10]. If the validation performance does not improve from one epoch to the following ones, the training stops.

2.4 Overfitting

One major risk against generalization is overfitting. Taking a human-like image, overfitting corresponds to a situation where the training consists of solely learning by heart a set of problem-solution. When a new problem arises, it does not match with any of the combinations that have been learnt. Therefore, the answer is mainly a guess, and may significantly deviate from the actual solution. The following briefly presents a few methods to prevent overfitting.

2.4.1 Regularization

Overfitting in ANNs typically results in large values for the weights. One way to avoid it is to implement regularization, which aims to add a penalty to the loss function if some weights become too large [10]. A commonly used method, the Bayesian regularization, consists of adding the sum of the squares of the weights to the loss function. The optimization of the loss function will therefore result in a balance between minimizing the error and minimizing the weights [12].

2.4.2 Cross-validation

In cross-validation, the learning process of a given ANN architecture is repeated several times, by changing the validation dataset [10]. In k-fold cross-validation, the learning dataset (training + validation) is divided into k subsets, and k iterations are performed by using each subset once for validation. Note that for cross-validation, the test dataset remains unchanged. The principle of cross-validation is illustrated in Figure 2.2.

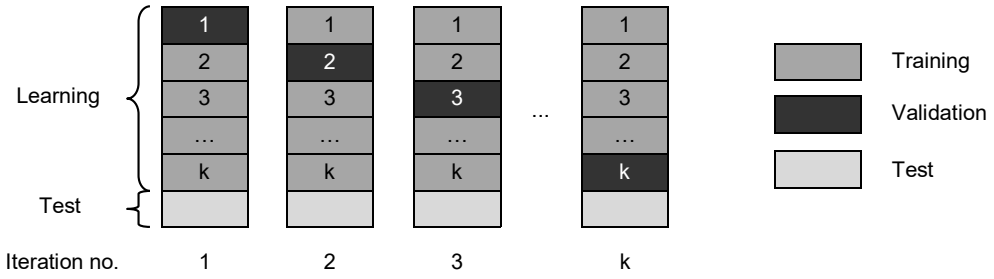

Figure 2.2: Principle of k-fold cross-validation

2.4.3 Early stopping

Early stopping consists in stopping the training after a limited number of iterations, i.e. before the loss function converges. This may result in a slightly reduced training performance, but it prevents the neural network from becoming overtrained.

2.5 Limitations

ANNs usually perform quite well for making predictions. However, because their structure is highly non-linear, it is still quite difficult to understand the reasoning behind the answer, i.e. the mathematical equation governing the outputs as a function of the inputs. This is a typical example of the trade-off that exists between interpretability and accuracy of the model in data analysis [9]. Therefore, one possibility is to implement a regression analysis apart from the ANN, which is easier to interpret but may be less accurate. Then, both performances can be compared, and one can assess whether the use of an ANN can significantly improve the accuracy of the prediction or not.

3. DATA COLLECTION

A literature review was made to collect data from accelerated mortar bar tests performed on a variety of SCMs. In order to compare the data on a fair basis, several criteria were applied for the data selection. First, the dataset was restricted to results obtained from a standard accelerated mortar bar test, i.e. ASTM C 1260/1567 or CAN/CSA A23.2-25A/28A. However, a tolerance was applied for tests where the w/b ratio was slightly modified (in most cases, 0.50 instead of 0.47 required).

Table 3.1: Overview of the dataset (*: origin not known)

Source	Type of SCM	Type and origin of aggregate	Number of datapoints
[8]	Fly ash class C & F, GGBF slag, Silica fume	River aggregate, Kızılırmak river (TUR)	119
[14]	Fly ash class C & F	Limestone, Spratt (CAN) Rhyolite, New Mexico (USA) Argillite, North Carolina (USA) Quartzite, South Dakota (USA)	40
[6]	Fly ash class C & F	Sand – Volcanic rock, Oregon (USA) 2 types of reactive sand, Texas (USA)	36
[15]	Fly ash class C & F	Reactive sand, *	34
[16]	Fly ash class C & F, Calcined clay	Rhyolite, Wyoming (USA) Reactive sand, Idaho (USA) Rhyolite – Andesite, New Mexico (USA) Glacial deposit - Shale, Iowa (USA)	32
[17]	Fly ash class C & F	Soda-lime glass sand, *	20
[7]	Fly ash class F, GGBF slag, Silica fume	2 types of reactive sand, Colombia	20
[18]	Calcined clay	Reactive sand, *	17
[19]	Silica fume	Limestone, Spratt (CAN)	16
[20]	Fly ash class C & F	River sand, Arkansas river (USA) with reactive sand (Jobe), El Paso (TX-USA)	16
[21]	Fly ash class F, GGBF slag, Silica fume	River sand, Ahmetli (TUR) Basaltic rock, Aliağa (TUR)	12
[22]	Fly ash class C, Natural pozzolan	Reactive sand, Texas (USA)	12
[23]	Metakaolin	Limestone, Spratt (CAN) Greywacke – Argillite, Sudbury (CAN)	8
[24]	Ground glass, Natural pozzolan	Rhyolite, Thailand	8
[25]	Crushed brick	River aggregate, *	7
[26]	Fly ash class C & F	Reactive sand, Briggs (TX-USA)	6
[27]	Fly ash class F	River aggregate, Sakarya river (TUR)	6
[28]	Metakaolin, Fly ash class C	Reactive sand, Texas (USA)	6
[29]	Fly ash class F	River aggregate, Aras river (IRN)	5
[30]	Natural pozzolan	River aggregate, *	5
[31]	Metakaolin	Basaltic rock, Aliağa (TUR)	5
[32]	Rice hush ash	Reactive sand, River Plate/Chaco (ARG)	5
[33]	Co-fired biomass ash	Reactive sand, Texas (USA)	5
[34]	Fly ash class C, Crushed brick	Perlite, Turkey	5
[35]	Ground glass	Reactive sand, *	4
[36]	Fly ash class C & F, Silica fume	Limestone, Spratt (CAN)	4
[37]	Metakaolin	Greywacke, Western Cape (ZAF)	4
[38]	GGBF slag	Reactive aggregate, Wawa (CAN)	4
[39]	Ground glass, Fly ash class C	Limestone, Spratt (CAN)	3
[40]	Fly ash class C	Reactive sand, Texas (USA)	3

The second criterion dealt with the expansion of the reference bars. The present paper focuses on the expansion obtained in the AMBT when using SCMs, and not on the reactivity of aggregates. Therefore, it was chosen to select tests only made with aggregates where the expansion of the reference test was larger than 0.2 % after 14 days of exposure. Finally, the materials were filtered from their chemical composition, in order to only keep tests where the contents in SiO_2, Al_2O_3, Fe_2O_3, MgO, CaO, SO_3 and Na_2O_{eq}, for both cement and SCM, are available. It was chosen to consider Na_2O_{eq} instead of Na_2O and K_2O separately to maximize the size of the dataset, as the distinct contents of Na_2O and K_2O were not always reported. In addition, SCMs for which the LOI was larger than 10 % or for which the sum of all seven constituents mentioned before was lower than 90 % were excluded.

This resulted in a selection of 92 different SCMs and a total of 467 data points. Note that the dataset included some tests performed with the same binder on different reactive aggregates. An overview of the dataset is presented in Table 3.1, and a ternary diagram of the materials is plotted in Figure 3.1.

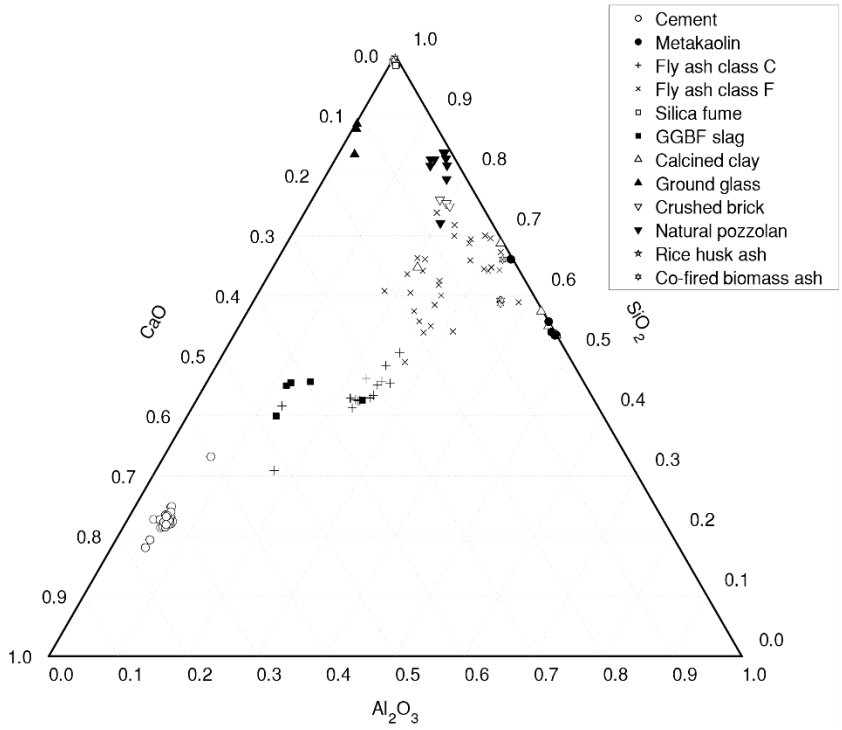

Figure 3.1: Ternary diagram of the selected materials

4. DATA ANALYSIS

The ANNs used for the present study were executed in MATLAB. Bayesian regularization combined with the Levenberg-Marquardt algorithm were implemented for the supervised training. The dataset was randomly divided into two subsets (85 % for learning, 15 % for test). The activation function was the sigmoid function, and the performance was assessed by calculating the mean square error.

4.1 Inputs

The inputs were derived from the partial chemical composition of the binder. The inclusion of one specific compound resulted in two values, namely the content by mass in the cement X_{cem} and in the SCM X_{SCM}. These values were then weighted by the replacement level RL according to Equation (5), so that x_{cem} and x_{SCM} were used as inputs for the model.

$$\begin{cases} x_{cem} = X_{cem} \cdot RL \\ x_{SCM} = X_{SCM} \cdot RL \end{cases} \quad (5)$$

It is desirable to have independent inputs for ANNs. However, when considering the chemical composition, the variables are strictly not independent, as their sum should be lower than 100 %. This is particularly true when considering the primary oxides, that account for the largest part of the composition usually.

Finally, input data were automatically normalized when using the *feedforwardnet* function in MATLAB.

4.2 Output

Since most data were from studies carried out with different aggregates, the expansion values obtained were not directly comparable. One way of overcoming this issue was to normalize the expansion y with the expansion of the associated reference test y_{ref}, as shown in Equation (6).

$$\hat{y} = \frac{y}{y_{ref}} \tag{6}$$

4.3 Choice of the architecture

Equation (4) gives a condition on the maximum number of hidden neurons. Given that the number of training data (68 % of 467, as the learning subset is divided into 5 for cross-validation, where each validation fold represents 17 % of the entire dataset – see the explanation in the next paragraph) was not extremely large, a factor 2 was applied to satisfy Equation (4), as shown per Equation (7).

$$H_{max} = \frac{1}{2}\frac{(N_{tr} - 1)\,O}{I + O + 1} \tag{7}$$

The choice of the architecture was based on a triple loop on the learning data subset only (Figure 4.1). The outer loop was an iteration on the number of hidden neurons, from 1 to H_{max}. The medium loop consisted of 30 iterations where the learning data subset was randomly divided for 5-fold cross-validation, therefore each fold corresponds to 17 % of the initial dataset. The same set of initial weights and biases was used for each iteration, the set being randomly selected prior to running the algorithm.

For each iteration, the termination was based on the validation performance: the training stopped when the mean square error (MSE) on the validation subset did not decrease for 8 epochs in a row.

The training and validation MSE were calculated for each iteration and averaged for the two inner loops. This resulted in a plot of both MSE as a function of the number of hidden neurons. These curves typically decrease and stabilize. However, if the number of hidden neurons is too larger, the MSE for validation may start to increase, which is a common sign of overtraining. The number of hidden neurons was finally selected as the minimum number of neurons for which the two MSE are less than 1 % higher than their minimum value. This is illustrated in Figure 4.1. Note that there were a few exceptions, where this criterion could not be fulfilled. In such a case, the tolerance was increased until finding an appropriate number of neurons.

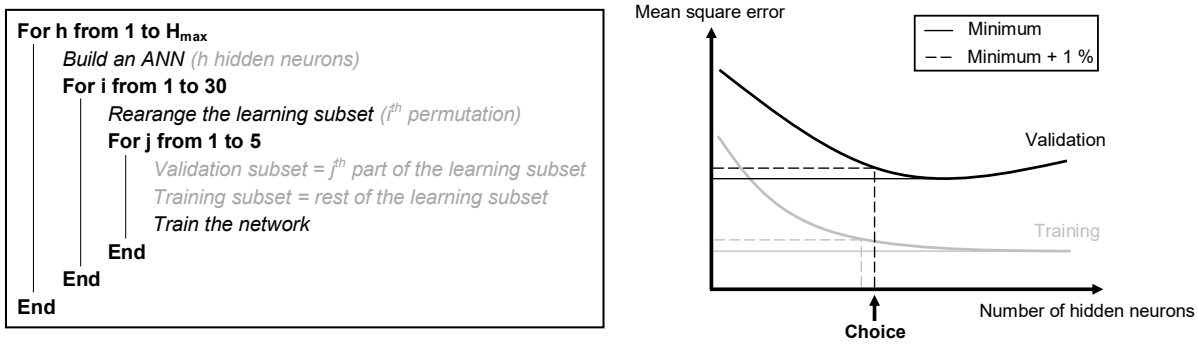

Figure 4.1: Triple loop algorithm (left) and schematic graph for selecting the number of hidden neurons (right)

4.4 Prediction

When the number of hidden neurons had been chosen, a new ANN was build based on the selected architecture. The new ANN was trained with the entire learning subset, i.e. the learning phase did not include any validation, in order to maximize the number of training data. In this case, early stopping was implemented to stop training, since the termination criterion used when choosing the architecture could no longer be applied. The maximum number of epochs corresponded to the average number of epochs performed during the choice of the architecture (i.e. after how many epochs the training stopped when performing cross-validation), for this specific number of neurons.

The results were split into the subset used for learning (85 % of the dataset) and the test subset (15 %). Note that before this stage, the test subset was not used at all, which made it ideal for making a final assessment of the neural network. For each subset, the coefficient of determination R^2 was calculated. The predictions were plotted against the experimental values in both cases. Besides, the residual errors were also displayed as a function of the replacement level. The residual error r was calculated based on Equation (8), where the subscripts p and m respectively stand for predicted and measured.

$$r = \widehat{y_p} - \widehat{y_m} \quad (8)$$

4.5 Variables

Since the objective of the present study was to investigate the effect of the chemical composition of the binder on the AMBT expansion, 12 different combinations of inputs were used. The baseline combination only included SiO_2 and CaO, as they were considered to have the largest effect on the test result [5, 6, 8]. In order to stress the influence of other compounds, 5 combinations were formed by adding a third oxide (Al_2O_3, Na_2O_{eq}, Fe_2O_3, MgO or SO_3) in addition to SiO_2 and CaO. In a similar way, 5 other combinations were created by including all oxides except one. Finally, the last combination to be tested included all seven compounds.

5. RESULTS

The chosen architecture and the performances obtained with the learning and the test subsets are given in Table 5.1, together with H_{max} calculated from Equation (7) and the selected number of neurons H.

Table 5.1: Architecture and performances of the ANN

Compounds selected for defining the inputs	Combination	H_{max}	H	Epochs	R^2 learning	R^2 test
SiO_2, CaO	1	27	10	34	0,824	0,896
SiO_2, CaO, Al_2O_3	2	20	8	31	0,852	0,879
SiO_2, CaO, Na_2O_{eq}	3	20	8	25	0,849	0,879
SiO_2, CaO, Fe_2O_3	4	20	8	34	0,853	0,901
SiO_2, CaO, MgO	5	20	6	27	0,837	0,906
SiO_2, CaO, SO_3	6	20	10	35	0,878	0,893
SiO_2, CaO, Na_2O_{eq}, Fe_2O_3, MgO, SO_3	7	11	7	30	0,909	0,873
SiO_2, CaO, Al_2O_3, Fe_2O_3, MgO, SO_3	8	11	7	33	0,897	0,915
SiO_2, CaO, Al_2O_3, Na_2O_{eq}, MgO, SO_3	9	11	7	30	0,912	0,902
SiO_2, CaO, Al_2O_3, Na_2O_{eq}, Fe_2O_3, SO_3	10	11	10	31	0,919	0,922
SiO_2, CaO, Al_2O_3, Na_2O_{eq}, Fe_2O_3, MgO	11	11	9	33	0,918	0,844
SiO_2, CaO, Al_2O_3, Na_2O_{eq}, Fe_2O_3, MgO, SO_3	12	10	7	31	0,915	0,914

Figure 6.1 shows the predicted normalized expansion plotted against the experimental normalized one for combination no. 12. The residual errors on the expansion as described per Equation (8), obtained with the same combination, are plotted against the cement replacement level in Figure 6.2.

6. DISCUSSION

Considering combination no.1 as the baseline, the addition of each single oxide (combinations no.2 to no.6 in Table 5.1) improved the performance of the ANN for learning. The smallest improvement was obtained when considering MgO, while the largest gain occurred with SO_3. These two observations were consistent with a previous analysis, where the MgO content of the binder was found to have a quite poor correlation with the normalized expansion, while the SO_3 content had the fourth best R^2 value behind SiO_2, CaO and Al_2O_3 [5].

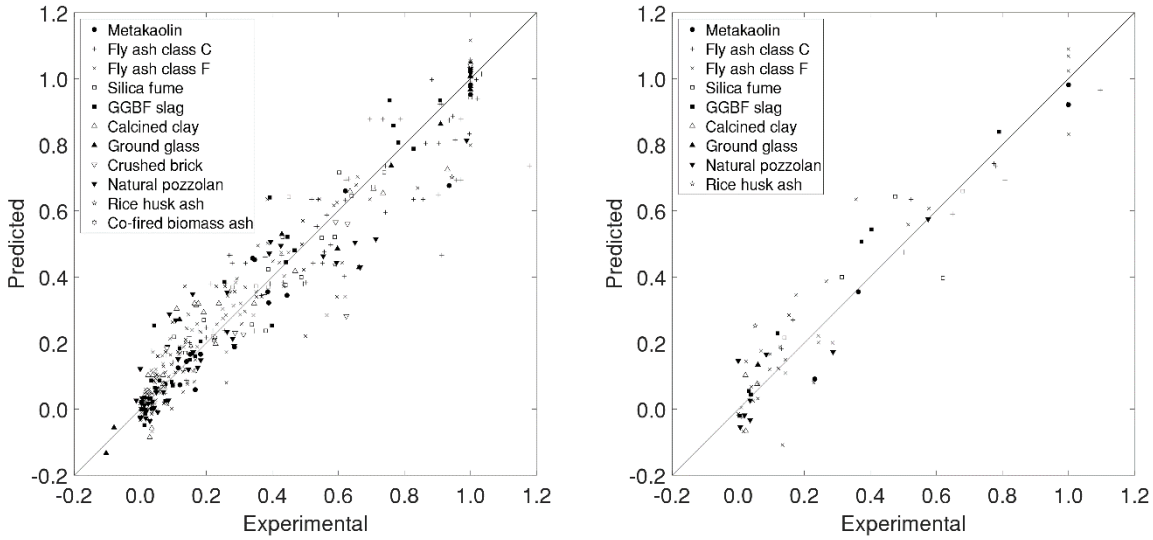

Figure 6.1: Predicted vs. experimental normalized expansion for the learning data subset (left) and the test data subset (right), for combination no.12. The black solid line is a one-to-one line

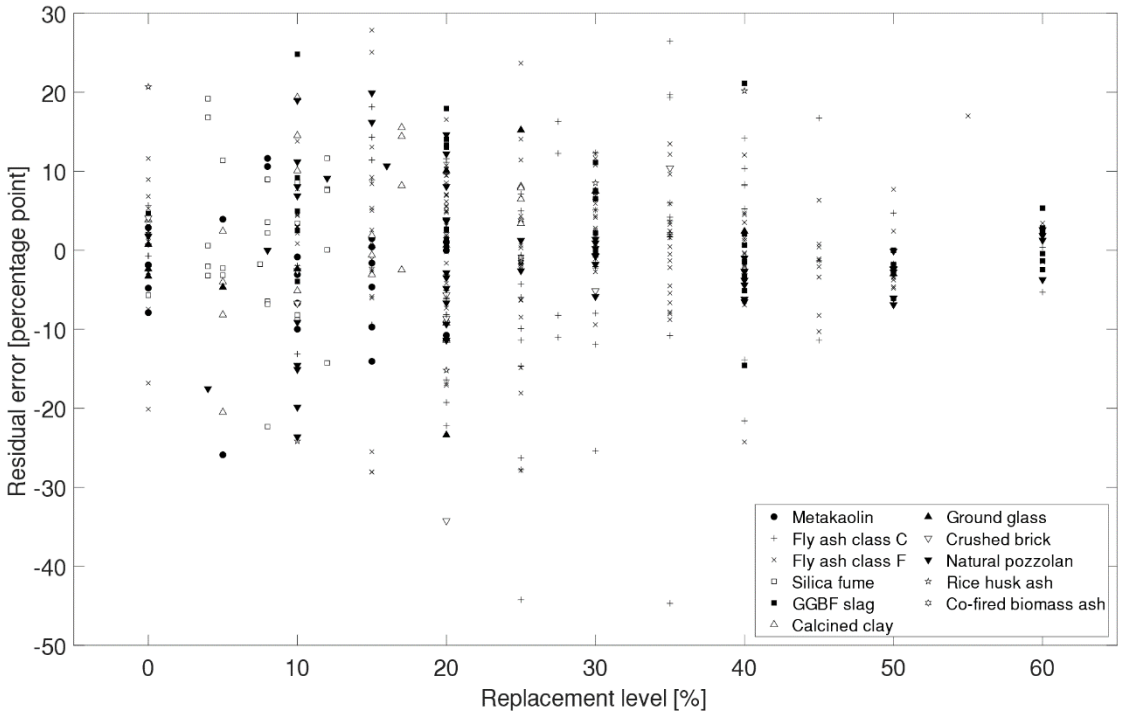

Figure 6.2: Residual error as a function of the replacement level for combination no.12

A reason for SO_3 to cause the best improvement in the present work could be due to a particularly large influence on a few datapoints, that where originally far away from the one-to-one line and strongly penalising the R^2 value. The ability of Na_2O_{eq} to improve the fitting is also worth to mention. Besides the very low R^2 value reported elsewhere [5], it is also known that the alkali concentration of the pore solution during the AMBT is dramatically changed due to alkali exchanges with the NaOH test solution [41], therefore it is not expected to see an influence from the alkali content of the binder. When considering the test subset, the influences were more variable, which could be due to some sampling effects. As the test subset was much smaller that the learning one, the R^2 value could be significantly modified by even fewer datapoints.

When combining all seven oxides (combination no.12), the performances were logically improved, both compared to the baseline and to the effect of each individual oxide. This can graphically be seen in Figure 6.1, where there is a clear trend for the results to match with the one-to-one line.

Combinations no.7 to no.11 were tested to further investigate the influence of each oxide on the performance. For almost all of them, the removal of one oxide caused no significant change in performance for the learning subset. One explanation to this behaviour could be that when increasing the number of oxides, the assumption of independence between the inputs becomes less and less valid. The only exception was seen for combination no. 8, where Na_2O_{eq} was removed. As mentioned before regarding combination no. 3, it was once again not expected that Na_2O_{eq} would influence the quality of the fitting. However, the exact effect of the alkali content on the expansion is not clear. Indeed, understanding the way ANNs process the inputs to predict the outputs is known to be a challenge. Numerous methods have been proposed to explain black box models [42], but it is still quite difficult to find the most appropriate technique for a given analysis.

The residual error plotted on Figure 6.2 shows the deviation of the prediction compared to the measured normalized expansion for combination no.12. Note that both subsets, learning and test, are combined on the figure. The average residual was 6.9 pp. (percentage point) for the learning subset, and 7.7 pp. for the test one. 53 % of the values were within ±5 pp. for the learning subset, 77 % within ±10 pp. and 94 % within ±20 pp.. This was respectively 43 %, 69 % and 94 % for the test subset. These results implied that in most cases, the ANN was able to predict the expansion reduction induced by the use of an SCMs, with an accuracy of 20 pp.. Although the accuracy was not high enough to predict the ability of an SCM to keep the expansion below 0.1 % at 14 days, it could be used as a screening tool in order to evaluate the potential of an SCM to perform well in the AMBT.

The largest differences were difficult to explain. However, most of them seemed to be related to the shape of the curve when plotting the expansion obtained in the AMBT as a function of the replacement level. It was seen that for some materials, the efficacy of the SCM is not linear, but is closer to an S-shaped curve: there is little to none reduction in expansion at low replacement levels, whereas the expansion is almost completely prevented at high replacement levels. This is for instance the case for one type of glass [24], one brick [34], on rice husk ash [32] and some class C fly ashes [6, 14, 16]. As a result, the ANN sometimes predicted an S-shape while the behaviour was rather linear, leading to an overestimation of the normalized expansion, but also sometimes behaved the other way around.

Finally, it should be mentioned that by increasing the size of the dataset, e.g. to a couple of thousand data, the consistency between the performances obtained on the learning and the test subsets would likely be improved, in particular by removing sampling effects and covering a broader range of materials.

7. CONCLUSION

Artificial neural networks bring new possibilities to analyse large datasets, especially when the input-output relationship is not well-established. The present work has shown that an ANN could be used as a screening tool with a relatively good accuracy to estimate the ability of an SCM to reduce the ASR expansion measured in the AMBT.

However, analysing the effect of each compound turned to be quite challenging. Although the addition of more inputs compared to CaO and SiO_2 alone had an evident benefit on the accuracy of the prediction, the quantitative evaluation of their impact remained unclear. Moreover, the assumption on the independence of the inputs may no longer be valid when increasing the number of inputs, as they are bound by an inequality (sum lower than 100 %). The present approach would probably benefit from using an even larger dataset, to widen the scope of materials and eliminate sampling effects. In parallel, investigating methods to extract knowledge from the ANN would help lifting the veil on the weaknesses of the model, although finding the most appropriate method is still challenging.

Finally, as the reliability of the prediction is closely related to the reliability of the input data, the choice of AMBT data can be questioned, particularly because the AMBT is far to be the best and appropriate test to evaluate effectiveness of SCMs against ASR. However, it should be noted that the present ANN model was designed to investigate the effect of the chemical composition of SCMs on the ASR expansion and did not aim to focus on a specific test method. In this respect the AMBT was chosen because, to the authors' knowledge, it offers the largest and most diverse dataset in the literature concerning SCMs and ASR expansion. Nevertheless, the model can easily be transposed to datasets obtained with other test methods such as the CPT or outdoor exposure blocks, as soon as a sufficient amount of data is available.

8. ACKNOWLEDGEMENTS

The authors gratefully acknowledge the financial support of Innovation Fund Denmark (Innovationsfonden) and Realdania for the present research project. We would also like to thank Line Clemmensen (DTU Compute) for the fruitful discussions and insights about artificial neural networks.

9. REFERENCES

1. Nielsen CV (2008) Carbon footprint of concrete buildings seen in the life cycle perspective. In: Proceedings NRMCA 2008 Concrete Technology Forum. pp 1–14
2. Rajabipour F, Giannini E, Dunant C, et al (2015) Alkali-silica reaction: Current understanding of the reaction mechanisms and the knowledge gaps. Cement and Concrete Research 76:130–146
3. Thomsen HCB, Grelk B, Barbosa RA, Hansen KK (2017) Alkali Release from Typical Danish Aggregates to Potential ASR Reactive Concrete. XXIIIth Symposium on Nordic Concrete Research & Development
4. Thomas M (2011) The effect of supplementary cementing materials on alkali-silica reaction: A review. Cement and Concrete Research 41:1224–1231
5. Malvar LJ, Lenke LR (2006) Efficiency of fly ash in mitigating alkali-silica reaction based on chemical composition. ACI Materials Journal 103:319–326
6. Schumacher KA, Ideker JH (2015) New Considerations in Predicting Mitigation of Alkali-Silica Reaction Based on Fly Ash Chemistry. Journal of Materials in Civil Engineering 27:04014144
7. Cassiani J, Dugarte M, Martinez-Arguelles G (2021) Evaluation of the chemical index model for predicting supplementary cementitious material dosage to prevent the alkali-silica reaction in concrete. Construction and Building Materials 275:
8. Mahyar M, Erdoğan ST, Tokyay M (2018) Extension of the chemical index model for estimating Alkali-Silica reaction mitigation efficiency to slags and natural pozzolans. Construction and Building Materials 179:587–597
9. James G, Witten D, Hastie T, Tibshirani R (2013) An Introduction to Statistical Learning - With application in R. Springer
10. Kim P (2017) MATLAB Deep Learning. Apress
11. Kamath U, Liu J, Whitaker J (2019) Deep Learning for NLP and Speech Recognition. Springer International Publishing
12. Livingstone DJ (2008) Artificial Neural Networks: Methods and Applications, Humana Press, Totowa, NJ
13. Yu H, Wilamowski BM (2018) Levenberg-Marquardt Training. In: Intelligent systems, CRC Press. pp 12–1
14. Rangaraju PR, Desai J (2009) Effectiveness of Fly Ash and Slag in Mitigating Alkali-Silica Reaction Induced by Deicing Chemicals. Journal of Materials in Civil Engineering 21:19–31
15. Kruse K, Jasso A, Folliard K, et al (2012) Characterizing Fly Ash, Report FHWA/TX-13/0-6648-1, Center for Transportation Research, University of Texas at Austin
16. Touma W, Fowler D, Carrasquillo R (2001) Alkali-silica reaction in Portland cement concrete: testing methods and mitigation alternatives. ICAR, Austin
17. Shafaatian SMH, Akhavan A, Maraghechi H, Rajabipour F (2013) How does fly ash mitigate alkali-silica reaction (ASR) in accelerated mortar bar test (ASTM C1567)? Cement and Concrete Composites 37:143–153
18. Li C, Ideker JH, Drimalas T (2015) The efficacy of calcined clays on mitigating alakli-silica reaction (ASR) in mortar and its influence on microstructure. RILEM Bookseries 10:211–217
19. Boddy AM, Hooton RD, Thomas MDA (2000) Effect of product form of silica fume on its ability to control alkali-silica reaction. Cement and Concrete Research 30:1139–1150
20. Phillips WJ (2015) Alkali Silica Reaction Mitigation Using High Volume Class C Fly Ash, Thesis and dissertations, University of Arkansas, Fayetteville
21. Yazıcı H, Beglarigale A, Tosun Felekoğlu K, Türkel S (2019) Comparing the alkali-silica reaction mitigation potential of admixtures by using different accelerated test methods. Construction and Building Materials 197:597–614

22. Cano RI (2013) Evaluation of Natural Pozzolans as Replacements for Class F Fly Ash in Portland Cement Concrete, MSc Thesis, The University of Texas at Austin
23. Ramlochan T, Thomas M, Gruber KA (2000) The effect of metakaolin on alkali-silica reaction in concrete. Cement and Concrete Research 30:339–344
24. Meesak T, Sujjavanich S (2019) Effectiveness of 3 different supplementary cementitious materials in mitigating alkali silica reaction. Materials Today: Proceedings 17:1652–1657
25. Turanli L, Bektas F, Monteiro PJM (2003) Use of ground clay brick as a pozzolanic material to reduce the alkali-silica reaction. Cement and Concrete Research 33:1539–1542
26. Shon CS, Sarkar SL, Zollinger DG (2003) Application of modified ASTM C1260 test for fly ash-cement mixtures. Transportation Research Record 1834:93–106
27. Yıldırım K, Sümer M (2014) Comparative analysis of fly ash effect with three different method in mortars that are exposed to alkali silica reaction. Composites Part B: Engineering 61:110–115
28. Moser RD, Jayapalan AR, Garas VY, Kurtis KE (2010) Assessment of binary and ternary blends of metakaolin and Class C fly ash for alkali-silica reaction mitigation in concrete. Cement and Concrete Research 40:1664–1672
29. Ahmadi B, Shekarchi M (2010) Use of natural zeolite as a supplementary cementitious material. Cement and Concrete Composites 32:134–141
30. Bektas F, Turanli L, Monteiro PJM (2005) Use of perlite powder to suppress the alkali-silica reaction. Cement and Concrete Research 35:2014–2017
31. Yazıcı Ş, Arel HŞ, Anuk D (2014) Influences of Metakaolin on the Durability and Mechanical Properties of Mortars. Arabian Journal for Science and Engineering 39:8585–8592
32. Rodríguez De Sensale G (2010) Effect of rice-husk ash on durability of cementitious materials. Cement and Concrete Composites 32:718–725
33. Shearer CR, Yeboah N, Kurtis KE, Burns SE (2012) Evaluation of biomass fired and co-fired fly ash for alkali-silica reaction mitigation in concrete. In: Drimalas T, Ideker JH, Fournier B (eds) Proceedings of the 14th International Conference on Alkali-Aggregate Reactivity in Concrete. Austin, TX, pp 10-pp
34. Bektas F (2007) Use of ground clay brick as a supplementary cementitious material in concrete-hydration characteristics, mechanical properties, and ASR durability, PhD Thesis, Iowa State University
35. Schwarz N, Cam H, Neithalath N (2008) Influence of a fine glass powder on the durability characteristics of concrete and its comparison to fly ash. Cement and Concrete Composites 30:486–496
36. Bérubé M-A, Duchesne J, Chouinard D (1995) Why the accelerated mortar bar method ASTM C1260 is reliable for evaluating the effectiveness of supplementary cementing materials in suppressing expansion due to alkali-silica reactivity. Cement Concrete and Aggregates 17:26–34
37. Bakera AT, Alexander MG (2018) Properties of Western Cape Concretes with Metakaolin. In: MATEC Web of Conferences. EDP Sciences
38. Hooton D, Donnelly CR, Clarida B, Rogers CA (2000) An assessment of the effectiveness of blast-furnace slag in counteracting the effects of alkali-silica reaction. In: Bérubé M-A, Durand B, Fournier B (eds) 11th International Conference on Alkali Aggregate Reaction. Québec City, pp 1313–1322
39. Shi C, Wu Y, Riefler C, Wang H (2005) Characteristics and pozzolanic reactivity of glass powders. Cement and Concrete Research 35:987–993
40. Shearer CR (2014) The productive reuse of coal, biomass and co-fired fly ash, PhD Thesis, Georgia Institute of Technology
41. Golmakani F, Hooton RD (2019) Impact of pore solution concentration on the accelerated mortar bar alkali-silica reactivity test. Cement and Concrete Research 121:72–80
42. Guidotti R, Monreale A, Ruggieri S, et al (2018) A survey of methods for explaining black box models. ACM Computing Surveys 51:1–42